NUCLEAR CALORIC CURVE

G. Raciti[1] for the ALADIN collaboration:
R. Bassini,[3] M. Begemann-Blaich,[2] S. Fritz,[2] S.J. Gaff,[8] C. Groß,[2] G. Immé,[4] I. Iori,[3] U. Kleinevoß,[2] G. J. Kunde,[8*] W.D.Kunze,[2] U. Lynen,[2] M. Mahi,[2] A. Moroni,[3] T. Möhlenkamp,[2†] W. F. J. Müller,[2] B. Ocker,[2] T. Odeh,[2] F. Petruzzelli,[3] J. Pochodzalla,[7] G.Riccobene,[1] F.P. Romano,[4] Th. Rubehn,[1‡] A. Sajia,[4] M. Schnittker,[2] A. Schüttauf,[2‡] C. Schwarz,[2] W. Seidel,[5] V. Serfling,[2] C. Sfienti,[1] W. Trautmann,[2] A. Trzcinski,[6] G. Verde,[4] A. Wörner,[2] H. Xi,[8] E. Zude,[1] B. Zwieglinski[6]

[1] *I.N.F.N.- Laboratorio Nazionale del Sud and Dipartimento di Fisica, Università di Catania, 44,via S.Sofia,I-95123 Catania, Italy*
[2] *Gesellschaft für Schwerionenforschung, D-64291 Darmstadt, Germany*
[3] *Dipartimento di Fisica, Università di Milano and I.N.F.N., I-20133 Milano, Italy*
[4] *Dipartimento di Fisica, Università di Catania and I.N.F.N., I-95129 Catania, Italy*
[5] *Forschungszentrum Rossendorf, D-01314 Dresden, Germany*
[6] *Soltan Institute for Nuclear Studies, 00-681 Warsaw, Hoza 69, Poland*
[7] *Max Planck Institut Heidelberg ,Saupfercheckweg 1,D-69177 Heidelberg, Germany*
[8] *National Superconducting Cyclotron Laboratory Michigan State University , East Lancing,MI 48824, USA*

Liquid-gas phase transition in nuclear matter is investigated via calorimetric studies. Nuclear calorimetry results obtained recently by the ALADIN collaboration are reported. In particular the so called "*nuclear caloric curve*" is analysed in details and a comparison of experimental data both from different heavy ion induced reactions, and different *temperature* measurements methods is discussed.

1 Introduction

The idea of a liquid-gas phase transition in nuclear matter [1,2],suggested by the Van der Waals behaviour of the nucleon-nucleon force, emerges from the experimentally proved existence of both phases: cold nuclear Fermi liquid and a nuclear gas consisting of free nucleons and a few light clusters. Nucleus-nucleus collisions at intermediate and relativistic energies have been shown [3] to be an ideal tool to produce pieces of finite nuclear matter at extremely different thermodynamical conditions. Excited nuclei disintegrate into many intermediate mass fragments (IMF) – i.e. fragments larger than evaporated particles and

*Present address: Yale University, New York, USA
†Present address: NSCL, Michigan State University, East Lansing, MI 48824
‡Present address: Max Planck Institut ,Germany

smaller than fission products or emission residues, signaling a phase transition, and at higher excitation energy into single nucleons [4] (*nuclear vapour*). To probe the phase diagram of a substance, the location of the critical point and the properties of the system around it, i.e. the critical exponents, as well as the boundaries between the liquid and the gas phase, must be investigated. While the question of criticality remains elusive [3], the exploration of the phase boundaries is possible via calorimetric studies. However the interpretation of caloric information on nuclei has to cope with several complications. Nuclei are finite, charged and small systems (as number of constituents) and, more important, they are transient systems where all the observables depend on time. Nevertheless it has been shown that for small H_2O cluster ($\sim$20 constituents) [5], the characteristic 'plateau' signaling the solid-to-liquid transition is still evident. This example rises the hope that finite hadronic systems may also exhibit sufficiently clear signatures of phase transitions.

2 How to produce nuclear samples at different phases

In order to analyse thermodynamical properties of nuclear systems we need to produce and select samples which deal with microcanonical ensembles at high excitation energies (in this limit microcanonical ensembles differ very little from grancanonical ones!)[7]. We can produce microcanonical nuclear samples either in head on collisions, where the excitation energy is determined by the incident beam energy, or in peripheral collisions at relativistic energies, where the spectator heating is controlled by the impact parameter.

In a series of experiments [6,8], projectile spectator multi-fragment decays have been studied with the ALADIN forward-spectrometer at SIS accelerator (GSI). The primary projectile spectator emerging from the abrasion phase is a well defined source which can be reconstructed on an event-by-event basis by looking at the phase space distribution of fragments, selected as belonging to its decay by the measured velocities. The same observables has been used to verify the isotropy of the fragment emission in the decaying spectator rest frame. When plotted against Z_{bound}, defined as the sum of the charges of all product nuclei with $Z \geq 2$ belonging to the spectator, the charge partition of fragmenting spectator nuclei shows no dependence on the entrance channel [6] (Fig.1). This loss of the memory signals an high degree of equilibration as confirmed by the very good agreement between statistical model calculations [9] and charge Z yields and higher order momenta of the Z - distribution of the emitted fragments [10,11]. The universal behaviour of the mean IMF multiplicity vs Z_{bound} with respect to the chosen target [8,12,10] ,projectile mass and incident energy [6] (Fig. 1) was termed the *rise and fall* of multi-fragment emission [12]

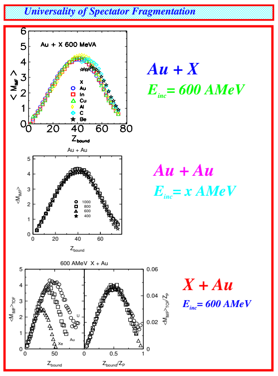

Figure 1: *Mean multiplicity of IMF (3$\leq$ Z $\leq$ 30) as a function of Z_{bound} for different combination of targets projectiles and energies*[6]*. Notice in the bottom right side the normalization to the atomic number Z_P of the projectile.*

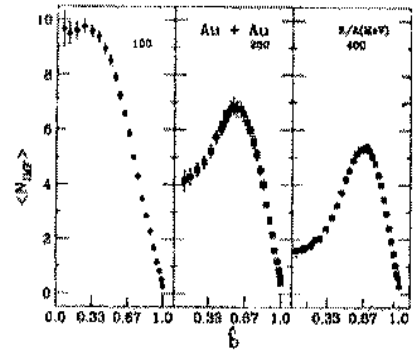

Figure 2: *N_{IMF} vs the impact parameter b deduced from particle multiplicities N_p.Notice that, small b correspond to large N_p values.*

because decreasing Z_{bound}, M_{IMF} increases up to a maximum at $Z_{bound}/Z_0 \approx$ 0.5 and then decrease at small Z_{bound}. Since Z_{bound} represents an estimate of the projectile size the decrease of M_{IMF} could be related to a smaller size of the system. The *rise and fall* of multifragment production was more clearly evidenced by studying central Au+Au collisions at E/A = 100,200,400 A$\cdot$MeV [4]. In these experiments participants decay was measured using the MSU–MINIBALL 4π detector. The $\langle M_{IMF}\rangle$ vs $\langle b\rangle$ are correlated in fig. 2. At small impact parameters b it is evident the decline of multifragmentation process at incident energies larger than 100 A$\cdot$MeV for systems with the same size. The multifragment production leaves the place to the vaporization of the system into single nucleons as far as enough excitation energy is stored on it. Fig. 3 shows some systematic results on this transition [6] and can be used as a recipe to produce nuclear systems in liquid, vapour and mixed phases.

3 How to measure excitation energy

In general, the excitation energy of the nuclear system, is measured by determining the invariant mass of the emitted fragments to compare to a nucleus in its groundstate (Q-values) and hence by summing up all their kinetic energies [13,14] in the decaying system rest frame.

Due to the large acceptance of the ALADIN-spectrometer to respect to the strong forward focusing of the projectile spectator fragments, nearly all of its decay products have been detected event-by-event and kinetic energies and masses have been measured. Hydrogen isotope contributions were estimated from the measured neutrons kinetic energies and multiplicities [14], masses when not directly measured, were estimated through the EPAX [15] parametrization. Nevertheless, recenlty [16] it has been shown that a nonnegligible fraction of the observed protons and nucleons kinetic energies is related with a preequilibrium emission and therefore should be excluded when the thermalized part of the excitation energy of the spectator is reconstructed. Fig. 4 shows the correlation

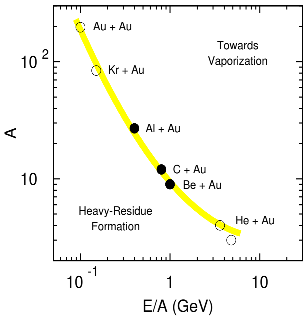

Figure 3: *Two-dimensional map of projectile mass versus bombarding energy*[6] *of reactions for which mean maximum IMF production has been observed in central collisions.*

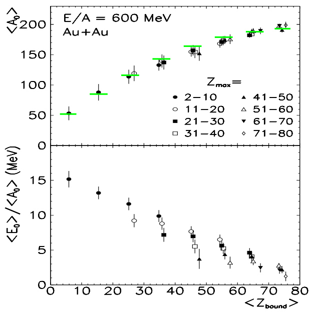

Figure 4: *Summed kinetic energies and masses of the different decay products of the projectile spectator as a function of* Z_{bound} *(from ref.* [14]*).*

between the decaying source mass and excitation energy to respect to Z_{bound}. In the framework of the *participant-spectators* model, the size of the projectile spectator depends on the impact parameter.Therefore Z_{bound} estimates at the same time both the spectator size and the total energy deposited in the participant region (*fire ball*). The increase of $\langle E/A \rangle$ for increasing centrality (small Z_{bound}) therefore shows that the spectator heating is mainly due to the energetic *fireball* nucleons.

When central collisions are selected, the system disintegrates completely into light fragments and particles making very difficult the excitation energy reconstruction. Moreover, an analysis of the charge distribution yields [17] and of the kinetic energy spectra [18] in these reactions has revealed a considerable collective outward motion superimposed on the random motion of the constituents at the breakup stage (radial flow). This feature prevails, with monotonously increasing flow values, over the range of bombarding energies up to 1000 MeV per nucleon [18,19,20]. A best fit of the data suggests a value of energy $E_{flow} = 0.4 \cdot E_{CM}$ that is not transferred to thermal degree of freedom [3].

4 How to measure temperature

Less straightforward is the determination of a nuclear temperature, since, for such small systems, we take recourse to statistical mechanics. For a micro-canonical ensemble the thermodynamic temperature may be defined in terms of the total-energy state density. But experimental observables of specific degrees-of-freedom can constitute a good approximation to the true thermodynamic temperature. Figure 5 illustrates three different methods to extract a temperature of an hadronic system [7]. The "*slope*" parameter method based

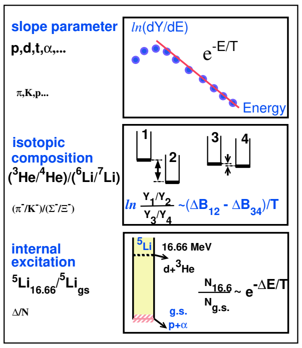

Figure 5: *Illustration of different thermometers for hadronic systems: inverse slope parameter (top part), isotope ratios (center part), and relative population of states (lower part).*

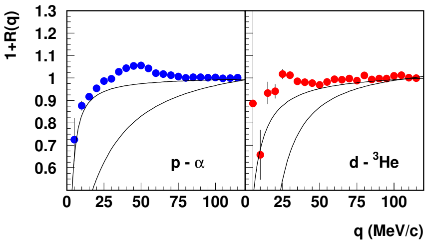

Figure 6: *Correlation functions for the ^{5}Li groundstate (left side) and the 16.7 MeV excited state (right side) in Au+Au collisions at 150 A·MeV. The solid lines represent the estimated background which, at small q, decreases due to the mutual Coulomb repulsion of the two charged particles.*

on maxwellian emission spectra, is known as the poorest one, if applied to not very selected spectra, due to the folding of preequilibrium emission. Isotope temperatures can be extracted from particle yields: assuming a nuclear system at low density and in chemical and thermal equilibrium a measure of the temperature T may be obtained via the double yield ratio of two isotope pairs, (Y_1/Y_2) and (Y_3/Y_4), differing by the same number of neutrons and/or protons [21]. Using the He and Li isotopes it follows that:

$$T_{HeLi,0} := 13.33/ln(2.18 \cdot \frac{Y_{6Li}/Y_{7Li}}{Y_{3He}/Y_{4He}}). \tag{1}$$

Remark that in Eq. 1 nuclei are considered in their ground state and secondary sequential decays of heavier fragments are ignored. In order to correct for this effect several systematic [22] and model dependent [23,3] studies has been reported. Despite the strong feeding of the light particle yields through secondary decays these first studies predict an almost linear dependence of $T_{HeLi,0}$ on the actual temperature T of the system (T= 1.2 $T_{HeLi,0}$). It must be noted, however, that the choice of the couple of the isotopes can reduce the sensitivity of this method [24]. On the other hand, the so called *emission temperature* can be deduced from coincidence measurements of the decay products [25]. The coincidence spectra, plotted as a function of the relative momentum of the two fragments, exhibit peaks due to resonance decay superimposed on the background of coincident but uncorrelated particle emission (Fig. 6).

From the acceptance corrected yields the nuclear temperatures may then be calculated via:

$$\frac{Y_1}{Y_2} = \frac{2J_1+1}{2J_2+1}\, e^{-\Delta E/T} \tag{2}$$

where Y_i, J_i are the yields and the spins of two states in the same isotope separated by the energy ΔE. This assumes that the states of the decaying fragments are populated according to a Boltzmann law. Also in this case additional corrections [28] are required by the feeding of the light fragments states from sequential decay of heavier fragments.

5 Nuclear caloric curve: experimental results

From the correlation of the measured temperature and excitation energy of the projectile spectators in ^{197}Au+^{197}Au collisions at 600 A·MeV a *caloric curve of nuclei* (Fig. 7) has recently been reported [14]. This caloric curve can be divided into three distinctly different sections. In line with previous studies in the fusion evaporation regime [29] the rise of T_{HeLi} for excitation energies below 2 MeV per nucleon is compatible with the low-temperature approximation of a fermionic system. Within the range of $\langle E_0\rangle/\langle A_0\rangle$ from 3 to 10 MeV, where multifragmentation regime dominates over fusion – evaporation process, an almost constant value for T_{HeLi} of about 4.5-5 MeV is observed. Finally,

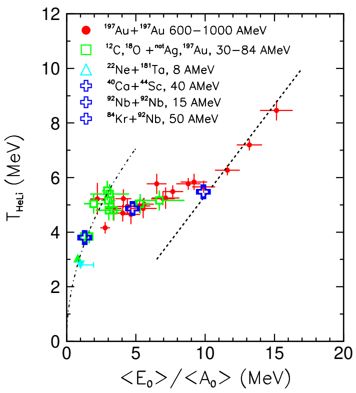

Figure 7: *Caloric curve of nuclei determined by the dependence of the isotope temperature T_{HeLi} on the excitation energy per nucleon.*

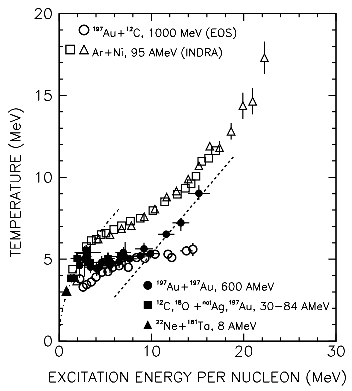

Figure 8: *Comparison of* ALADIN*'s caloric curve (solid points) to the EOS collaboration* [26] *(open circles),for spectators, and INDRA collaboration* [27] *(open triangles and squares) , for quasi-projectile.*

beyond a total excitation energy of 10 MeV per nucleon, a steady rise of T_{HeLi} with increasing $\langle E_0\rangle/\langle A_0\rangle$ is seen.

The similarity of this curve to first-order liquid-gas phase transitions in macroscopic systems has initiated a widespread discussion which addresses both methodical aspects and question of interpretation. Therefore, in order to check experimental methods we have performed new experiments in which the temperatures were deduced simultaneously both from the yield of stable isotopes (isotope temperatures) and from the population of excited states (emission temperatures).

The symmetric Au + Au system was studied at the SIS accelerator at GSI. We used seven telescopes around the target to allow isotope identification of fragments up to Z=5 and three large area Si-CsI hodoscopes with fine granularity that allow to reconstruct the yield of particle unstable states from the correlation functions of their decay products. With this set-up [30] we studied:
- at 1000A·MeV incident energy the target spectator fragmentation. To reduce contributions from the fireball the hodoscopes were placed at backward angles with respect to the beam axis.
- at incident energies between 50 and 200A·MeV, the interaction region in cen-

tral collisions. In this case the hodoscopes covered the region around 90^0 in the CM-system where contributions from possible remnants of the projectile and target should be minimal.

At 1000 A·MeV the impact parameter was deduced from Z_{bound} [12] of the projectile – spectator. For the investigation of the interaction region only a coarse determination of the impact parameter was sufficient, since the degree of centrality affects mainly the size of this source whereas the excitation energy per nucleon is determined by the incident energy. In particular we estimated excitation energies as the total available center-of-mass energy subtracted of the radial flow, as an upper limit.

In both cases a similar range of excitation energies is covered, although most other parameters of the reactions, e.g. flow or source size are very different. It should, therefore, be possible to investigate the influence of these parameters on the measured temperatures.

5.1 Isotope thermometer

The isotope temperatures T_{HeLi}, measured from the target spectators fragments in the Au+Au reaction at 1000 A · MeV, are in a very good agreement (fig. 7) with the previous values obtained for the projectile spectators. Because of the Z_{bound} selection on projectile products, the observed agreement represents an autocorrelation free methodical test. Figure 8 summarizes the presently available caloric curves measured via T_{HeLi} as defined in Eq. 1. A recent result of the EOS collaboration for $^{197}Au+^{12}C$ central collisions at 1000 A·MeV beam energy is shown by the open circles [26]. These data nicely confirm the plateau-like behaviour at intermediate excitation energies between 5 and 10 MeV per nucleon, though the rise at high excitation energies is not observed in that experiment. From the recent results on the projectile fragmentation in the Ar+Ni collisions at 95 A·MeV [27](INDRA collaboration), compared to our data, the temperatures appear to be systematically higher by about 1-2 MeV. However, also these data show an upswing at an excitation energy of about 10 MeV per nucleon. Clearly, more systematic studies are needed in order to clarify whether these discrepancies are due to the definition of the decaying source (which in the Fermi-energy regime is not well separated from the fireball), the size of the system or the different chemical composition (N/Z) of the source.

In order to test the size dependence of the caloric curve we studied Kr+Nb collisions at 35, 70, 100, 120 A·MeV and Ar+Sc at 50, 100, 150 A·MeV at the NSCL facility of the MSU with a setup very similar to that of ref. [30]. The 4π MSU SOCCER BALL was used as multiplicity filter. Ca+Sc collisions at 40A·MeV and Nb+Nb at 15 A·MeV were studied at the CS accelerator of the

LNS (Catania).

The preliminary values we extracted for the isotope temperature in Kr+Nb, Ca+Sc and Nb+Nb collisions from *quasi-central* selected events, look consistent with our previous results (Fig. 7); in particular these data nicely confirm the plateau-like behaviour at excitation energies between 5 and 10 A·MeV for decaying systems masses ranging from almost 80 to 200 mass units.

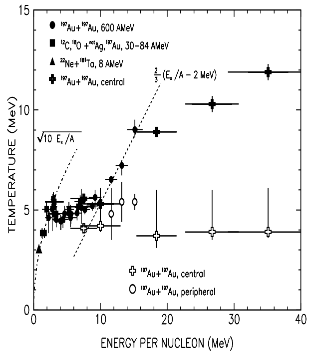

Figure 9: *Comparison of isotope temperatures T_{HeLi} (closed symbols) with emission ones (open symbols).*

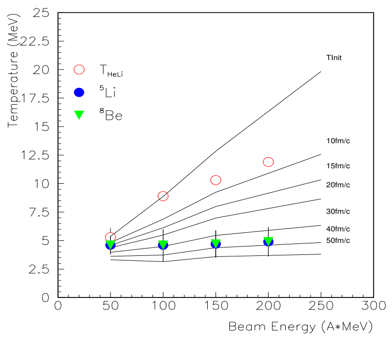

Figure 10: *Adiabatic expansion of an ideal gas.*

5.2 "Isotope" and "emission" temperatures and cooling of hot nuclei

The cross comparison of the *isotope* temperature with the *emission* one, over a large excitation energy region has been already analysed for the Au+Au reactions but not yet for the other quoted systems. Typical experimental correlation functions for ^{5}Li fragment decay to the ground and excited (16.7 MeV) states are shown in Fig. 6. In fig. 9 isotope and emission temperatures from ^{5}Li decay are compared. For peripheral collisions we notice a slightly increasing discrepancy between the two thermometers. Both look consistent again if one apply the correction due to the secondary decay feeding [22]. For central collisions the differences between the two thermometers show up very pronounced. With increasing beam energy the isotope temperatures are rising, whereas the emission temperatures remain constant. Secondary decay corrections cannot explain this difference and other explanations have to be found. If we follow the time evolution of a heated nucleus isoentropically expanding from nuclear saturation density, in the framework of the EES model[31], an enhanced emission of ^{4}He nuclei and IMF relative to the other light particles, emitted earlier,is predicted when the source has expanded to a minimum of the density (at t $\approx$ 60fm/c). As a consequence, light particles (including ^{3}He) sample the temporal evolution of the expanding source with different time-dependent weights than IMF and ^{4}He nuclei do. This emission at different stages of the reactions, while adds complexity to the meaning of "*isotope temperatures*" involving ^{3}He and ^{4}He isotopes ,has been used to explain the different shapes of the kinetic energy spectra of light particles and alphas[32,33]. In particular the high energy tail in the spectra of ^{3}He and H isotope emitted from the Au target spectator at 1000 A·MeV[33] can be ascribed to higher temperature stages.

For illustration, we will turn to an adiabatic expanding ideal gas (Fig. 10). Starting within a given volume and, taking into account the radial flow energy, is observed that, while the isotope temperatures reflect the temperature at the first stages of the expanding system, the ^{5}Li temperatures recall the system in the last stage of the adiabatic process.

6 Concluding remarks

Disentangling collective and thermal motion in fireball generated in central collisions, one observes a similar caloric behaviour as in spectator fragmentation at high excitation energies. This concordance suggests that, despite the very different underlying kynematics, the multifragment decays in both reaction types may be governed by common physics.

The shape of the caloric curve is suggestive of a first-order phase transition with a substantial latent heat but is no longer characterized by a singular point, opening the possibility to a coesistent second order phase transition[34].

The time evolution of the multifragmentation process in terms of different degrees-of-freedom freeze out at various stages, recalls a similar phenomenon during the cosmic big-bang evolution. Since in the latter this cooling is intimately related to the existence of collective radial flow, it may not be too surprising that the discrepancy between the isotope and emission thermometers arises at beam energies where collective radial flow becomes important. While the different energy dependence of the two thermometers can be explained by different freeze-out condition (*i.e. time*) and might enable us to sample the cooling curve of the system, it clearly exemplifies that we are still far away from a detailed understanding of the thermodynamics of a finite nucleus decaying into quantum clusters.

References

1. H. Jaqaman *et al.*, *Phys. Rev.* C **29**, 2067 (1984).
2. P.J. Siemens, *Nature* **305**, 410 (1983).
3. J. Pochodzalla, *Prog. Part. Nucl. Phys.* **39**, 443 (1997).
4. M.B. Tsang *at al.*, *Phys. Rev.* C **53**, 1959 (1996).
5. D.J. Wales and I. Ohmine, *J. Chem. Phys.* **98**, 7245 (1993).
6. A. Schüttauf *et al.*, *Nucl. Phys.* A **607**, 457 (1996).
7. D.J. Morissey, *et al.*, *MSU-Report* 922 F66 1994.
8. J. Hubele *et al.*, *Phys. Rev.* C **46**, R1577 (1992).
9. J.P.Bondorf *et al.*, Phys. Rep. 257 (1995) 133
10. P. Kreutz *et al.*, *Nucl. Phys.* A **556**, 672 (1993).
11. A.S. Botvina *et al.*, *Nucl. Phys.* A **584**, 737 (1995)
12. C.A. Ogilvie *et al.*, *Phys. Rev. Lett.* **67**, 1214 (1991).
13. X. Campi *et al.*, *Phys. Rev.* C **50**, R2680 (1994).
14. J. Pochodzalla *et al.*, *Phys. Rev. Lett.* **75**, 1040 (1995).
15. K.Sümmerer *et al.*, *Phys. Rev.* C **42**, 2546 (1990).
16. U. Lynen *et al.*,*Proceedings of the 6^{th} Int. Conf. on Nucleus-Nucleus Collisions* -Gatlinburg,Tennessee (USA) June 1997 .
17. G.J. Kunde *et al.*, *Phys. Lett.* B **272**, 202 (1991).
18. W.C. Hsi *et al.*, *Phys. Rev. Lett.* **73**, 3367 (1994).
19. G. Poggi *et al.*, *Nucl. Phys.* A **586**, 755 (1995).
20. M.A. Lisa *et al.*, *Phys. Rev. Lett.* **75**, 2662 (1995).
21. S. Albergo *et al.*, *Nuovo Cimento A* **89**, 1 (1985).
22. M.B. Tsang *et al.*, *Phys. Rev.* C **53**, R1057 (1996).
23. D.H.E. Gross *et al.*, *Phys. Rev. Lett.* **56**, 1544 (1986); D.H.E. Gross, *Prog. Part. Nucl. Phys.* **30**, 155 (1993).
24. F. Gulminelli and D. Durand, *Nucl. Phys.* A **615**, 117 (1997).
25. J. Pochodzalla *et al.*, *Phys. Rev.* C **35**, 1695 (1987).
26. J.A. Hauger *et al.*, *Phys. Rev. Lett.* **77**, 235 (1996).
27. Y.G. Ma *et al.*, LPC pre-print LPCC 96-10 (1996).
28. C. Schwarz *et al.*, *Phys. Rev.* C **49**, 3316 (1994).
29. D. Fabris *et al.*, *Phys. Lett.* B **196**, 429 (1987) and references therein.
30. G. Immé *et al.*, *Proceedings of the 1st CRIS'96: Critical Phenomena and Collective Observables*, World Scientific, p. 143 (1996).
31. W.A. Friedman, *Phys. Rev.* C **42**, 667 (1990).
32. R. Bougault *et al.*,*Proceedings of the 35th International Winter Meeting on Nuclear Physics*, Bormio, Italy, January 1997 pag. 251
33. H. Xi *et al.*, *Z. Phys.* A (in print)1997.
34. J.B. Elliott *et al.*, *Phys. Rev.* C **49**, 3185 (1994).